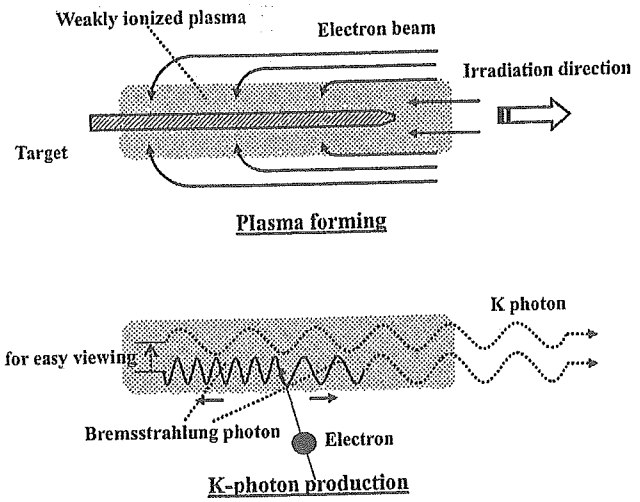

Fig. 4 K-photon irradiation from weakly ionized plasma.

sequently, Kβ rays (8.90 keV) are absorbed effectively using a 10-μm-thick nickel K-edge filter with an edge of 8.33 keV, and quite clean Kα rays (8.04 keV) are produced.

3 Characteristics

3.1 *Tube Voltage and Current*

Tube voltage and current were measured by a high-voltage divider with an input impedance of 1 GΩ and a current transformer, respectively. Figure 5 shows the time relation for the tube voltage and current. At the indicated charging voltages, they roughly displayed damped oscillations. When the charging voltage was increased, both the maximum tube voltage and current increased. At a charging voltage of 50 kV, the maximum tube voltage was almost equal to the charging voltage of the main condenser, and the maximum tube current was approximately 15 kA.

3.2 *X-Ray Output*

An x-ray output pulse was detected using a combination of a plastic scintillator and a photomultiplier using a 10-μm-thick monochromatic copper filter (Fig. 6). The x-ray pulse height substantially increased with corresponding increases in the charging voltage. The x-ray pulse widths were about 700 ns, and the time-integrated x-ray intensity per pulse measured by a thermoluminescence dosimeter (Kyokko TLD Reader 1500 utilizing MSO-S elements without energy compensation) had a value of about 20 μC/kg at 1.0 m from the x-ray source, with a charging voltage of 50 kV.

3.3 *X-Ray Source*

To measure images of the Kα source, we employed a pinhole camera with a hole diameter of 100 μm (Fig. 7). When the charging voltage was increased, the plasma x-ray source grew, and both spot dimension and intensity increased. Because the x-ray intensity is the highest at the center of the spot, both the dimension and intensity decreased according to both increases in the thickness of a filter for absorbing x-rays and decreases in the pinhole diameter.

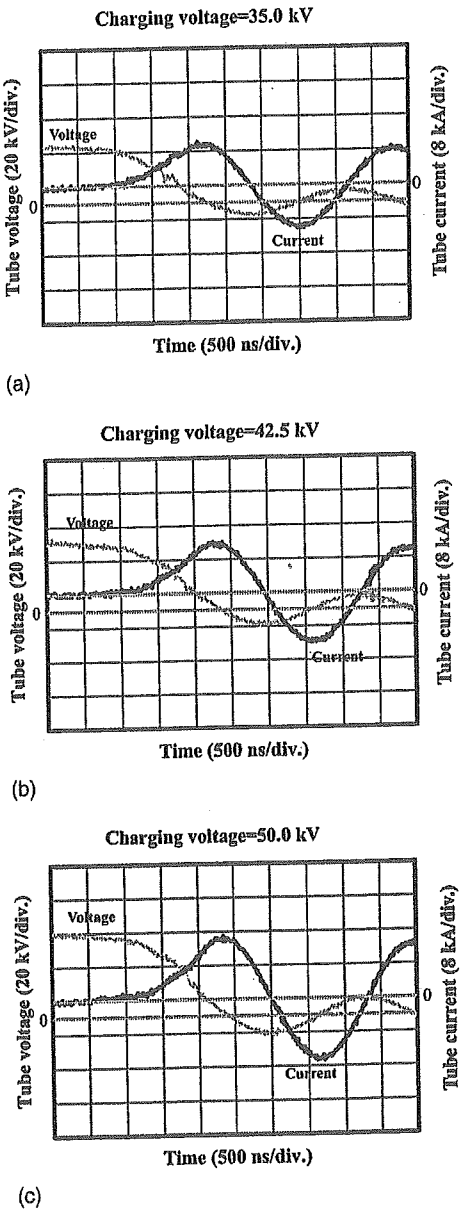

Fig. 5 Tube voltages and currents with charging voltage of (a) 35.0 kV, (b) 42.5 kV, and (c) 50.0 kV.

3.4 *X-Ray Spectra*

X-ray spectra from the plasma source were measured using a transmission-type spectrometer with a lithium fluoride

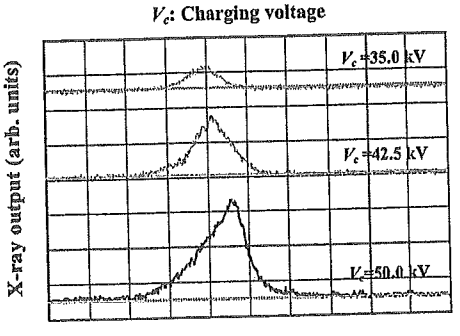

Fig. 6 X-ray outputs measured by plastic scintillator with changes in charging voltage.

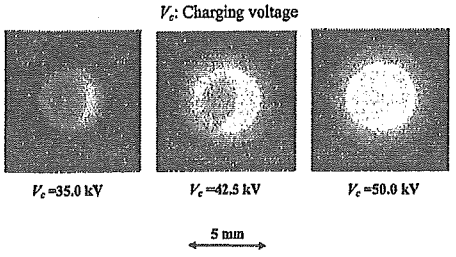

Fig. 7 Images of Kα x-ray source measured by pinhole of 100 μm from plasma axial direction.

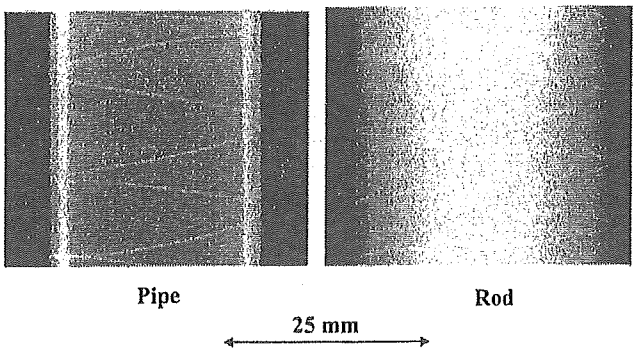

Fig. 9 Radiograms of tungsten wires 50 μm in diameter coiled around pipe, and rod made of polymethyl methacrylate.

curved crystal 0.5 mm in thickness. The spectra were taken by a computed radiography (CR) system[21] (Konica Regius 150) with a wide dynamic range, using the filter, and relative x-ray intensity was calculated from Dicom digital data. Figure 8 shows measured spectra from the copper target using the filter. In fact, we observed clean Kα lines such as lasers, and confirmed the significant filtering effect, while bremsstrahlung rays were hardly detected at all. The characteristic x-ray intensity of the Kα lines substantially increased with corresponding increases in the charging voltage, and the Kβ line was absorbed by the filter. Although this spectrometer has sufficient energy resolution for measuring Kα_1 and Kα_2 lines, we could observe only a single line.

4 Radiography

Plasma radiography was performed by the CR system without using the filter, and the distance between the x-ray source and imaging plate was 1.2 m.

First, rough measurements of image resolution were made using wires. Figure 9 shows radiograms of 50-μm-diam tungsten wires coiled around a pipe, and a rod made of polymethyl methacrylate with a charging voltage of 50 kV. Although the image contrast increased using the pipe, 50-μm-diam wires could be observed.

The image of water falling into a polypropylene beaker from a glass test tube is shown in Fig. 10. This image was taken with a charging voltage of 45 kV, with the slight addition of an iodine-based contrast medium. Because the x-ray duration was about 1 μs, the stop-motion image of water could be obtained.

Figure 11 shows an angiogram of a rabbit heart; iodine-based microspheres of 15 μm in diameter were used with a charging voltage of 50 kV, and fine blood vessels of about 100 μm were visible.

5 Discussion

Concerning the spectrum measurement, we obtained fairly clean Kα lines from a weakly ionized linear plasma x-ray

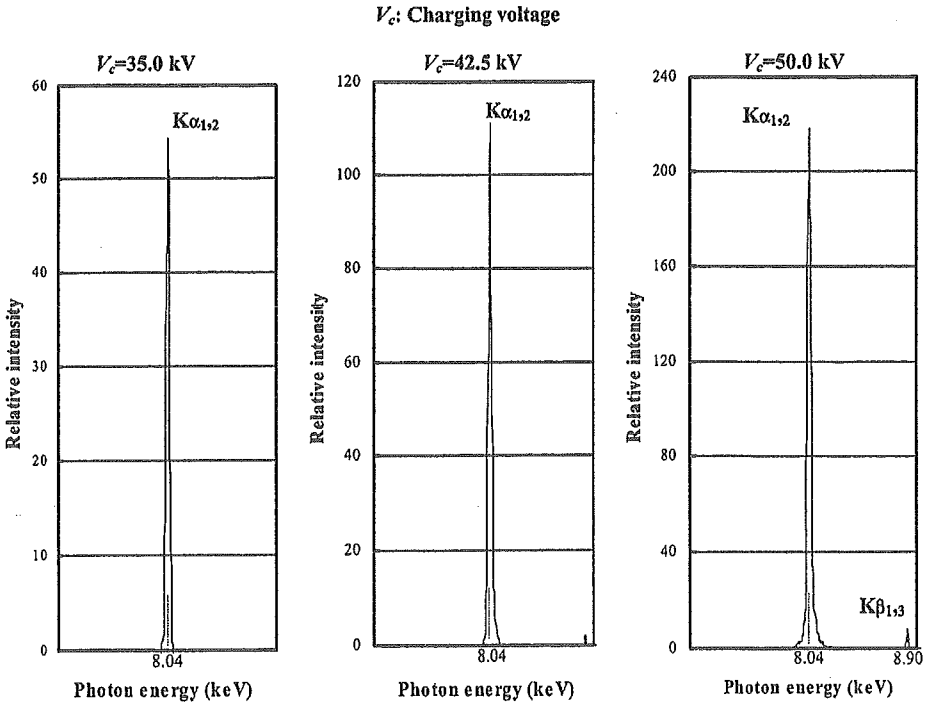

Fig. 8 X-ray spectra from weakly ionized copper plasma according to changes in charging voltage and to insertion of nickel K-edge filter.

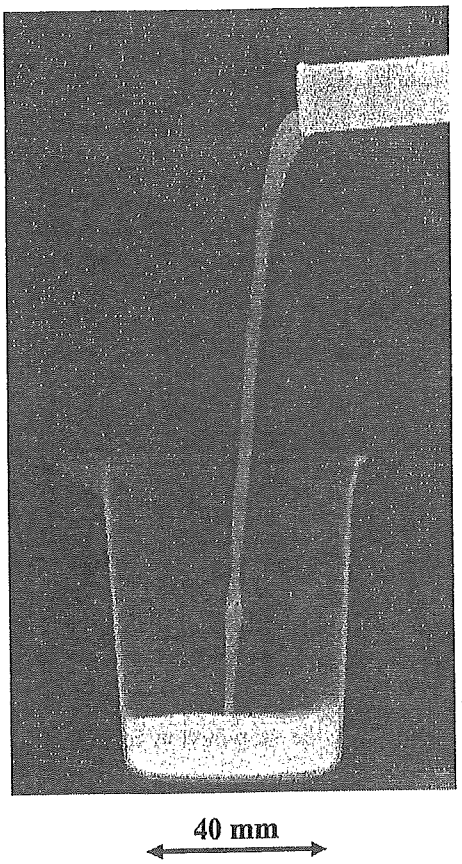

Fig. 10 Radiogram of water falling into polypropylene beaker from glass test tube.

source by absorbing $K\beta$ lines using the K-edge filter. The lines are produced by x-ray enhancement by spontaneous emission, and the coherence can be increased by development of a resonator or by pulse laser irradiations from the plasma axial direction to produce higher harmonics. In a medical application, cerium $K\alpha$ rays (34.6 keV) are absorbed effectively by an iodine-based contrast medium, and high contrast microangiography can be performed.

In this research, we obtained sufficient characteristic x-ray intensity per pulse for CR radiography using the filter, and the generator-produced number of characteristic $K\alpha$ photons was approximately 5×10^{13} photons/cm$^2\cdot$s at 1.0 m from the source. In addition, since the photon energy of characteristic x-rays can be controlled by changing the target elements, various quasimonochromatic high-speed

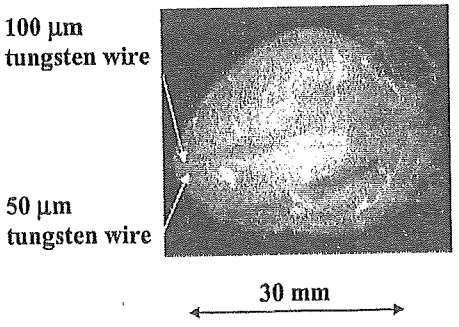

Fig. 11 Angiograms of rabbit heart.

radiographies, such as high-contrast microangiography and parallel radiography using an x-ray lens, will be possible.

Acknowledgments

This work was supported by Grants-in-Aid for Scientific Research (13470154, 13877114, and 16591222) and Advanced Medical Scientific Research from MECSST; Health and Labor Sciences Research Grants (RAMT-nano-001, RHGTEFB-genome-005, and RHGTEFB-saisei-003); and grants from Keiryo Research Foundation, The Promotion and Mutual Aid Corporation for Private Schools of Japan, Japan Science and Technology Agency (JST), and New Energy and Industrial Technology Development Organization (NEDO, Industrial Technology Research Grant Program in 2003).

References

1. A. Mattsson, "Some characteristics of a 600 kV flash x-ray tube," *Phys. Scr.* **5**, 99–102 (1972).
2. R. Germer, "X-ray flash techniques," *J. Phys. E* **12**, 336–350 (1979).
3. C. Cavailler, "AIRIX—a new tool for flash radiography in detonics," *Proc. SPIE* **4183**, 23–35 (2000).
4. E. Sato, H. Isobe, and F. Hoshino, "High intensity flash x-ray apparatus for biomedical radiography," *Rev. Sci. Instrum.* **57**, 1399–1408 (1986).
5. E. Sato, M. Sagae, K. Takahashi, T. Oizumi, H. Ojima, K. Takayama, Y. Tamakawa, T. Yanagisawa, A. Fujiwara, and K. Mitoya, "High-speed soft x-ray generators in biomedicine," *Proc. SPIE* **2513**, 649–667 (1994).
6. E. Sato, M. Sagae, K. Takahashi, A. Shikoda, T. Oizumi, H. Ojima, K. Takayama, Y. Tamakawa, T. Yanagisawa, A. Fujiwara, and K. Mitoya, "Dual energy flash x-ray generator," *Proc. SPIE* **2513**, 723–735 (1994).
7. E. Sato, M. Sagae, A. Shikoda, K. Takahashi, T. Oizumi, M. Yamamoto, A. Takabe, K. Sakamaki, Y. Hayasi, H. Ojima, K. Takayama, and Y. Tamakawa, "High-speed soft x-ray techniques," *Proc. SPIE* **2869**, 937–955 (1996).
8. E. Sato, S. Kimura, S. Kawasaki, H. Isobe, K. Takahashi, Y. Tamakawa, and T. Yanagisawa, "Repetitive flash x-ray generator utilizing a simple diode with a new type of energy-selective function," *Rev. Sci. Instrum.* **61**, 2343–2348 (1990).
9. S. Kimura, E. Sato, M. Sagae, A. Shikoda, T. Oizumi, K. Takahashi, Y. Tamakawa, and T. Yanagisawa, "Disk-cathode flash x-ray tube driven by a repetitive two-stage Marx pulser," *Med. Biol. Eng. Comput.* **31**, S37–S43 (1993).
10. A. Shikoda, E. Sato, M. Sagae, T. Oizumi, Y. Tamakawa, and T. Yanagisawa, "Repetitive flash x-ray generator having a high-durability diode driven by a two-cable-type line pulser," *Rev. Sci. Instrum.* **65**, 850–856 (1994).
11. E. Sato, K. Takahashi, M. Sagae, S. Kimura, T. Oizumi, Y. Hayasi, Y. Tamakawa, and T. Yanagisawa, "Sub-kilohertz flash x-ray generator utilizing a glass-enclosed cold-cathode triode," *Med. Biol. Eng. Comput.* **32**, 289–294 (1994).
12. K. Takahashi, E. Sato, M. Sagae, T. Oizumi, Y. Tamakawa, and T. Yanagisawa, "Fundamental study on a long-duration flash x-ray generator with a surface-discharge triode," *Jpn. J. Appl. Phys.* **33**, 4146–4151 (1994).
13. J. J. Rocca, V. Shlyaptsev, F. G. Tomasel, O. D. Cortazar, D. Hartshorn, and J. L. A. Chilla, "Demonstration of a discharge pumped table-top soft x-ray laser," *Proc. Phys. Lev. Lett.* **73**, 2192–2195 (1994).
14. J. J. Rocca, D. P. Clark, J. L. A. Chilla, and V. N. Shlyaptsev, "Energy extration and achievement of the saturation limit in a discharge-pumped table-top soft x-ray amplifier," *Phys. Lev. Lett.* **77**, 1476–1479 (1996).
15. C. D. Macchietto, B. R. Benware, and J. J. Rocca, "Generation of millijoule-level soft-x-ray laser pulses at a 4-Hz repetition rate in a highly saturated tabletop capillary discharge amplifier," *Opt. Lett.* **24**, 1115–1117 (1999).
16. J. J. G. Rocca, J. L. A. Chilla, S. Sakadzic, A. Rahman, J. Filevich, E. Jankowska, E. C. Hammarsten, B. M. Luther, H. C. Kapteyn, M. Murnane, and V. N. Shlyapsev, "Advances in capillary discharge soft x-ray laser research," *Proc. SPIE* **4505**, 1–6 (2001).
17. E. Sato, Y. Suzuki, Y. Hayashi, E. Tanaka, H. Mori, T. Kawai, K. Takayama, H. Ido, and Y. Tamakawa, "High-intensity quasi-monochromatic x-ray irradiation from the linear plasma target," *Proc. SPIE* **4505**, 154–164 (2001).
18. E. Sato, Y. Hayasi, E. Tanaka, H. Mori, T. Kawai, T. Usuki, K. Sato, H. Obara, T. Ichimaru, K. Takayama, H. Ido, and Y. Tamakawa,

"Quasi-monochromatic radiography using a high-intensity quasi-x-ray laser generator," *Proc. SPIE* **4682**, 538–548 (2002).
19. E. Sato, Y. Hayasi, R. Germer, E. Tanaka, H. Mori, T. Kawai, H. Obara, T. Ichimaru, K. Takayama, and H. Ido, "Irradiation of intense characteristic x-rays from weakly ionized linear molybdenum plasma," *Jpn. J. Med. Phys.* **23**, 123–131 (2003).
20. E. Sato, Y. Hayasi, R. Germer, E. Tanaka, H. Mori, T. Kawai, T. Ichimaru, K. Takayama, and H. Ido, "Quasi-monochromatic flash x-ray generator utilizing weakly ionized linear copper plasma," *Rev. Sci. Instrum.* **74**, 5236–5240 (2003).
21. E. Sato, K. Sato, and Y. Tamakawa, "Film-less computed radiography system for high-speed Imaging," *Ann. Rep. Iwate Med. Univ. Sch. Lib. Arts Sci.* **35**, 13–23 (2000).

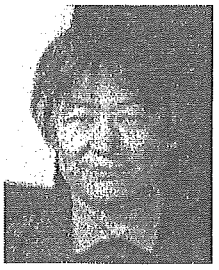

Eiichi Sato received his BS, MS, and PhD in applied physics from Tohoku Gakuin University, Sendai, Japan, in 1979, 1982, and 1987, respectively. From 1982, he was an assistant in the Department of Physics, and became as associate profrssor in 1986. Since 2004, he has been a professor of Physics at Iwate Medical University. He has written some 400 publications and delivered some 200 international presentations concerning x rays. His research interests include soft flash x-ray generators, quasi-x-ray laser generators, and high-speed radiography. In 2000 he received the Schardin Gold Medal from the German Physical Society, and in 2003 he received the Takayama Award (Gold Medal) from the Japan Society of High Speed Photography and Photonics.

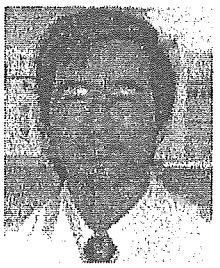

Etsuro Tanaka received his MD and PhD degrees in medicine from Kumamoto University, Japan, in 1980 and 1986, respectively. He worked on medical image processing in the Department of Physiology, Tokai University, Japan, from 1988 to 2003. He is currently a professor in the Department of Nutritional Sciences, Tokyo University of Agriculture, Japan. His research interests include medical image processing, human physiology, and clinical nutrition.

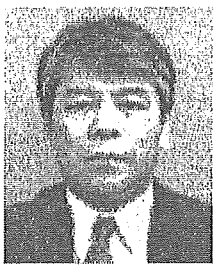

Hidezo Mori received a medical degree from Keio University School of Medicine, Tokyo, Japan, in 1977, and also a PhD from the Post Graduate School, Keio University School of Medicine. Now he is the Director of the Department of Cardiac Physiology at the National Cardiovascular Center, Suita, Japan. His primary research interests are regenerative therapy in cardiovascular disease, microcirculation, and medical applications of structural biology.

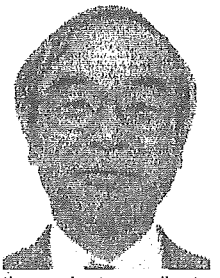

Toshiaki Kawai received the BS degree in precision mechanics and the MS degree in electronic engineering from Shizuoka University, Hamamatsu, Japan in 1964 and 1974, respectively. In 1974, he joined the Hamamatsu Photonics K.K., where he worked on research and development of solid-state infrared detectors, and then from 1978 to 1981 engaged in research work on the NEA cold cathode for application to imaging camera tubes. He is now the project coordinator of the Electron Tube Division #2 and is engaged in the development and manufacturing of imaging devices and x-ray equipment. He is a member of the Japan Radioisotope Association and the Institute of Image Information and Television Engineers of Japan.

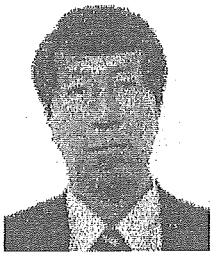

Shigehiro Sato received his MD degree from Iwate Medical University in 1980. He worked for the laboratory of the Division of Pediatric Infectious Diseases at Johns Hopkins Hospital from 1985 to 1989. He is currently a professor in the Department of Microbiology at Iwate Medical University. His research interests include central nervous system damage caused by Vero toxin, a cell culture system for vaccine development, and microangiography.

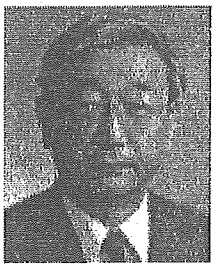

Kazuyoshi Takayama received his BS degree from Nagoya Institute of Technology in 1962. In 1970, he received his PhD in mechanical engineering from Tohoku University. Since 1986, he has been a director (professor) of the Shock Wave Research Center, Institute of Fluid Science, Tohoku University. His research interests include various shock wave phenomena, high-speed photography, and flash radiography. He has received seven awards including the coveted Ernst Mach Medal in 2000.

Myocardial interstitial choline and glutamate levels during acute myocardial ischaemia and local ouabain administration

T. Kawada,[1] T. Yamazaki,[2] T. Akiyama,[2] T. Shishido,[1] H. Mori[2] and M. Sugimachi[1]

1 *Department of Cardiovascular Dynamics, National Cardiovascular Center Research Institute, Osaka, Japan*

2 *Department of Cardiac Physiology, National Cardiovascular Center Research Institute, Osaka, Japan*

Received 25 November 2004, accepted 16 March 2005
Correspondence: T. Kawada, Department of Cardiovascular Dynamics, National Cardiovascular Center Research Institute, 5-7-1 Fujishirodai, Suita, Osaka 565-8565, Japan.
E-mail: torukawa@res.ncvc.go.jp

Abstract

Aim: Noradrenaline (NA) uptake transporters are known to reverse their action during acute myocardial ischaemia and to contribute to ischaemia-induced myocardial interstitial NA release. By contrast, functional roles of choline and glutamate transporters during acute myocardial ischaemia remain to be investigated. Because both transporters are driven by the normal Na^+ gradient across the plasma membrane in a similar manner to NA transporters, the loss of Na^+ gradient would affect the transporter function, which would in turn alter myocardial interstitial choline and glutamate levels. The aim of the present study was to examine the effects of acute myocardial ischaemia and the inhibition of Na^+,K^+-ATPase on myocardial interstitial glutamate and choline levels.

Methods: In anaesthetized cats, we measured myocardial interstitial glutamate and choline levels while inducing acute myocardial ischaemia or inhibiting Na^+,K^+-ATPase by local administration of ouabain.

Results: The choline level was not changed significantly by ischaemia (from 0.93 ± 0.06 to 0.82 ± 0.13 μM, mean ± SE, $n = 6$) and was decreased slightly by ouabain (from 1.30 ± 0.06 to 1.05 ± 0.07 μM, $P < 0.05$, $n = 6$). The glutamate level was significantly increased from 9.5 ± 1.9 to 34.7 ± 6.1 μM by ischaemia ($P < 0.01$, $n = 6$) and from 8.9 ± 1.0 to 15.9 ± 2.3 μM by ouabain ($P < 0.05$, $n = 6$). Inhibition of glutamate transport by *trans*-L-pyrrolidine-2,4-dicarboxylate (*t*-PDC) suppressed ischaemia- and ouabain-induced glutamate release.

Conclusion: Myocardial interstitial choline level was not increased by acute myocardial ischaemia or by Na^+,K^+-ATPase inhibition. By contrast, myocardial interstitial glutamate level was increased by both interventions. The glutamate transporter contributed to glutamate release via retrograde transport.

Keywords acetylcholine, cardiac microdialysis, cats, coronary artery occlusion, myocardium, noradrenaline.

Acute myocardial ischaemia causes oxygen depletion and loss of ATP in the ischaemic region (Hearse 1979). Blockade of H^+-ATPase leads to noradrenaline (NA) leakage from storage vesicles and axoplasmic NA accumulation (Schömig *et al.* 1988). Intracellular acidosis causes Na^+ influx via Na^+/H^+ exchange. Inhibition of Na^+,K^+-ATPase activity reduces the Na^+ gradient across the plasma membrane. Because NA uptake transporters are driven by the normal Na^+ electrochemical gradient across the plasma membrane,

axoplasmic NA accumulation and reduction of the Na^+ gradient cause reverse transport of NA from the intracellular space to the extracellular space (Schwartz 2000). Acute myocardial ischaemia evokes the myocardial interstitial NA release in the ischaemic region via retrograde NA transport, independently of efferent sympathetic nerve activity (Schömig *et al.* 1984, Yamazaki *et al.* 1996, Akiyama & Yamazaki 1999, Kawada *et al.* 2001a).

Similar to NA, choline and glutamate are taken up into cells by plasma membrane transporters driven by the Na^+ gradient (Schwartz 2000). We hypothesized that the loss of Na^+ gradient under ischaemic conditions would interfere with the transporter function, which would in turn alter myocardial interstitial choline and glutamate levels. Choline release has been suggested as an index of ischaemic degradation of the myocardial phospholipid bilayer in isolated, Tyrode solution-perfused rat hearts (Brühl *et al.* 2004). Glutamate can be a preferred myocardial fuel during ischaemia and may have protective effects on ischaemic myocardium (Arsenian 1998). Measuring myocardial interstitial levels of these molecules *in vivo* would contribute to understanding the pathophysiology of acute myocardial ischaemia. To test the hypothesis, we employed an *in vivo* cardiac microdialysis technique and measured myocardial interstitial choline and glutamate levels in anaesthetized cats (Akiyama *et al.* 1991, 1994, Yamazaki *et al.* 1997, Kawada *et al.* 2001b). Acute myocardial ischaemia inevitably affects systemic haemodynamics and perfusion of the heart. To minimize such haemodynamic effects, we also examined the effects of Na^+,K^+-ATPase inhibition on the myocardial interstitial choline and glutamate levels by locally administering ouabain through a dialysis probe (Yamazaki *et al.* 1999, Kawada *et al.* 2002). The results of the present study indicated that the myocardial interstitial choline level was not increased by acute myocardial ischaemia or by Na^+,K^+-ATPase inhibition. By contrast, the myocardial interstitial glutamate level was increased by both interventions. The glutamate transporter contributed to glutamate release via retrograde transport.

Materials and methods

Surgical preparation

Animal care was conducted in strict accordance with the *Guiding Principles for the Care and Use of Animals in the Field of Physiological Sciences* approved by the Physiological Society of Japan. Adult cats weighing 2.0–4.8 kg were anaesthetized via an intraperitoneal injection of pentobarbital sodium (30–35 mg kg^{-1}) and ventilated mechanically with room air mixed with oxygen. The depth of anaesthesia was maintained with a continuous intravenous infusion of pentobarbital sodium (1–2 mg kg^{-1} h^{-1}) through a catheter inserted via the right femoral vein. Mean systemic arterial pressure was monitored from a catheter inserted via the right femoral artery.

With the animal in the lateral position, the left fifth and sixth ribs were resected to expose the heart. When a coronary occlusion was necessary, a 3-0 silk suture was prepared around the left anterior descending coronary artery (LAD) just distal to the first diagonal branch. With a fine guiding needle, a dialysis probe was implanted into the left ventricular free wall perfused by the LAD. Heparin sodium (100 U kg^{-1} bolus injection followed by a maintenance dose of 50 U kg^{-1} h^{-1}) was administered intravenously to prevent blood coagulation. At the end of the experiment the experimental animals were killed by an overdose of pentobarbital sodium. We confirmed that the dialysis probe had been implanted within the left ventricular myocardium.

Dialysis technique

We designed a transverse dialysis probe (Akiyama *et al.* 1991, 1994). For measurements of small molecular compounds including ACh, choline, and glutamate, we used a dialysis fibre of 50 000 molecular weight cutoff (13 mm length, 310 μm OD, 200 μm ID; PAN-1200, Asahi Chemical, Osaka, Japan) with both ends glued to polyethylene tubes (20 cm length, 500 μm OD, 200 μm ID). The dialysis probe was perfused at a rate of 2 μL min^{-1} with Ringer solution. Each sample was collected in a microtube containing 3 μL of phosphate buffer (100 mM, pH 3.5). A cholinesterase inhibitor eserine (100 μM) was added to the perfusate to measure ACh. A preliminary examination indicated that whether the perfusate-contained eserine did not affect myocardial interstitial choline levels significantly. Dead space volume between the dialysis fibre and the sample microtube was identical for ACh, choline, and glutamate measurements, and the sampling was performed taking into account the time for dialysate to traverse the dead space volume.

The dialysate ACh and choline levels were measured directly by high-performance liquid chromatography with electrochemical detection. The absolute detection limits of ACh and choline, determined with a signal-to-noise ratio of 3, were 10 and 5 fmol per injection, respectively. The dialysate glutamate level was measured by kinetic enzymatic analysis with CMA 600. The absolute detection limit of glutamate was 1 μM per injection.

Protocols

All protocols were started from 2 h after implanting the dialysis probe. To examine changes in myocardial

interstitial ACh and choline levels during acute myocardial ischaemia ($n = 6$), after collecting a 15-min baseline dialysate sample, we occluded the LAD for 60 min and obtained four consecutive 15-min dialysate samples. The full-length of the implanted dialysis fibre was located within the ischaemic area judged by discoloration of myocardium during the LAD occlusion. We then released the occlusion and collected a 15-min dialysate sample during reperfusion. To examine changes in myocardial ACh and choline levels in response to local ouabain administration ($n = 6$), after collecting a 15-min baseline dialysate sample, we replaced the perfusate with Ringer solution containing 100 μM ouabain and collected four consecutive 15-min dialysate samples.

In different groups of animals, myocardial interstitial glutamate levels were measured during acute myocardial ischaemia ($n = 6$) and during local administration of ouabain ($n = 6$). To elucidate the role of the glutamate transporter, we also examined the effects of glutamate transport inhibition by *trans*-L-pyrrolidine-2,4-dicarboxylate (*t*-PDC, 10 mM) on myocardial interstitial glutamate levels during acute myocardial ischaemia ($n = 7$) and local administration of ouabain ($n = 7$). *t*-PDC was locally administered through the dialysis probe to avoid systemic effects.

Statistical analysis

All data are presented as mean ± SE values. In each protocol, the effects of myocardial ischaemia or local ouabain administration were examined using one-way analysis of variance followed by Dunnett's test against the corresponding baseline level (Glantz 2002). The baseline as well as maximum glutamate levels with and without glutamate transport inhibition were compared by an unpaired *t*-test during acute myocardial ischaemia or during local ouabain administration (Glantz 2002). Differences were considered to be significant when $P < 0.05$.

Results

Figure 1a shows myocardial interstitial ACh level during acute myocardial ischaemia. The ACh level was increased by LAD occlusion, becoming approximately 15 times higher than the baseline level at 30–45 and 45–60 min of ischaemia. The ACh level decreased towards the baseline level upon reperfusion. Figure 1b illustrates myocardial interstitial choline level during acute myocardial ischaemia. The choline level did not change significantly throughout the ischaemic and reperfusion periods.

Figure 2a shows changes in myocardial interstitial ACh level during local administration of ouabain. The ACh level was increased by the inhibition of

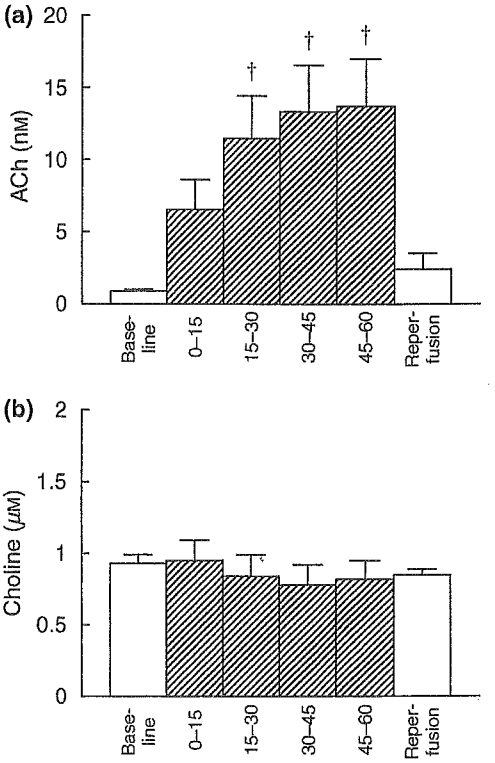

Figure 1 Changes in myocardial interstitial acetylcholine (ACh) level (a) and choline level (b) during coronary artery occlusion and reperfusion. Myocardial interstitial ACh level was significantly increased by acute myocardial ischaemia, while myocardial interstitial choline level was not changed. Data are mean ± SE. †$P < 0.01$ from baseline.

Na^+,K^+-ATPase, becoming approximately nine times higher than the baseline level at 15–30 min. The ACh level then decreased but remained significantly higher than the baseline level. Figure 2b illustrates the myocardial interstitial choline level during local administration of ouabain. The choline level was significantly lower at 0–15 and 45–60 min when compared with the baseline level.

Figure 3a shows changes in myocardial interstitial glutamate level during acute myocardial ischaemia. LAD occlusion increased the glutamate level to approximately 3.5 times higher than the baseline level at 0–15 min. Thereafter, the glutamate level was significantly higher than the baseline level throughout the ischaemic and reperfusion periods. Figure 3b illustrates the effects of glutamate transport inhibition on the ischaemia-induced glutamate release. The baseline glutamate level was significantly decreased by glutamate transport inhibition ($P < 0.05$). Although acute myocardial ischaemia and reperfusion significantly increased the glutamate level relative to the baseline level, the maximum glutamate level was attenuated to approximately one-fifth compared with that observed without glutamate transport inhibition ($P < 0.05$).

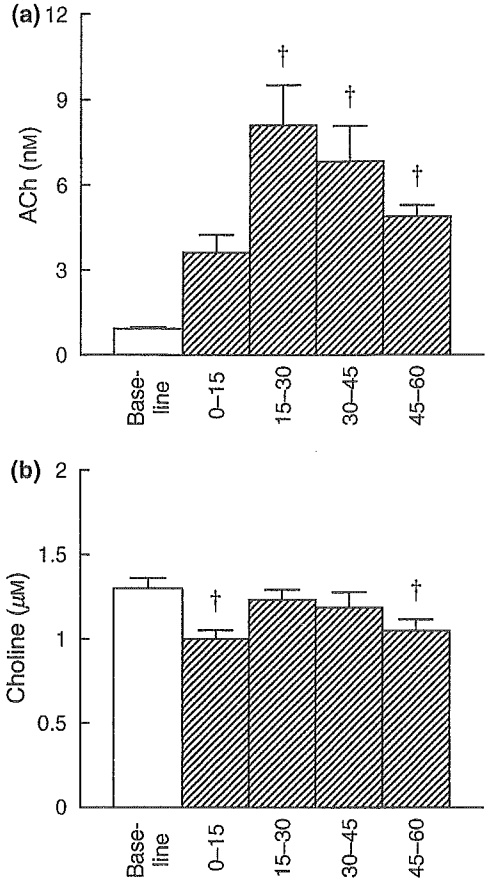

Figure 2 Changes in myocardial interstitial acetylcholine (ACh) level (a) and choline level (b) in response to the local administration of ouabain. Myocardial interstitial ACh level was significantly increased by ouabain. In contrast, myocardial interstitial choline level was decreased by ouabain. Data are mean ± SE. †$P < 0.01$ from baseline.

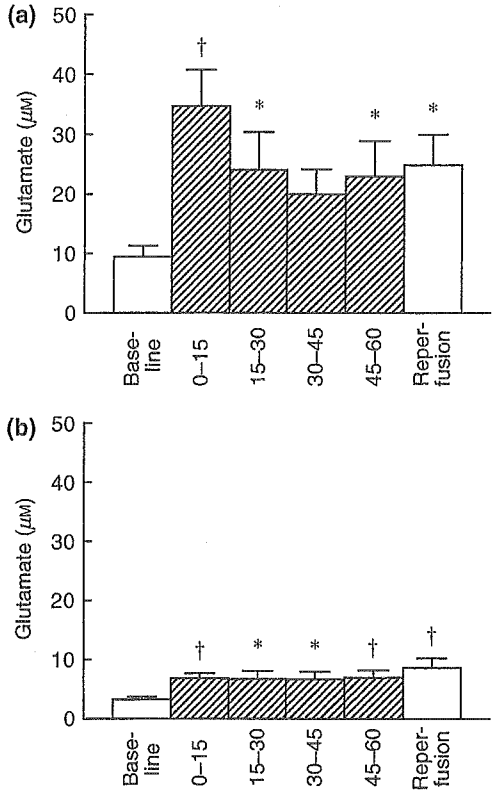

Figure 3 Changes in myocardial interstitial glutamate level during coronary artery occlusion and reperfusion without (a) and with (b) the inhibition of glutamate transporter. The glutamate level was significantly increased by acute myocardial ischaemia. The ischaemia-induced glutamate release was suppressed by the inhibition of glutamate transporter. Data are mean ± SE. †$P < 0.01$ and *$P < 0.05$ from baseline.

Figure 4a shows changes in myocardial interstitial glutamate level during the local administration of ouabain. Ouabain administration did not change the glutamate level at 0–15 min but increased the glutamate level thereafter. The glutamate level became approximately 1.8 times higher than the baseline level at 30–45 min. Figure 4b illustrates the effects of glutamate transport inhibition on ouabain-induced glutamate release. The baseline glutamate level was significantly decreased by the inhibition of glutamate transport ($P < 0.05$). Although ouabain administration increased the glutamate level relative to the baseline level, the maximum glutamate level was suppressed to approximately one-third of that observed without glutamate transport inhibition ($P < 0.05$).

Discussion

We have shown that acute myocardial ischaemia and local inhibition of Na^+,K^+-ATPase increased myocardial interstitial glutamate level but not choline level. Despite the similar Na^+ gradient dependency of corresponding transporters, myocardial interstitial glutamate and choline levels showed differential responses to the two interventions.

Changes in myocardial interstitial choline level

In the vagal nerve endings, ACh is hydrolysed to acetate and choline by acetylcholinesterase (Nicholls 1994). Choline is then taken up into the vagal nerve endings by the choline transporter driven by the Na^+ gradient. We hypothesized that loss of Na^+ gradient during acute myocardial ischaemia or local ouabain administration would increase the myocardial interstitial choline level by the interruption of choline uptake. Contrary to our hypothesis, acute myocardial ischaemia did not change myocardial interstitial choline level in the ischaemic region (Fig. 1b). Ouabain administration decreased the myocardial interstitial choline level at 0–15 and 45–60 min (Fig. 2b).

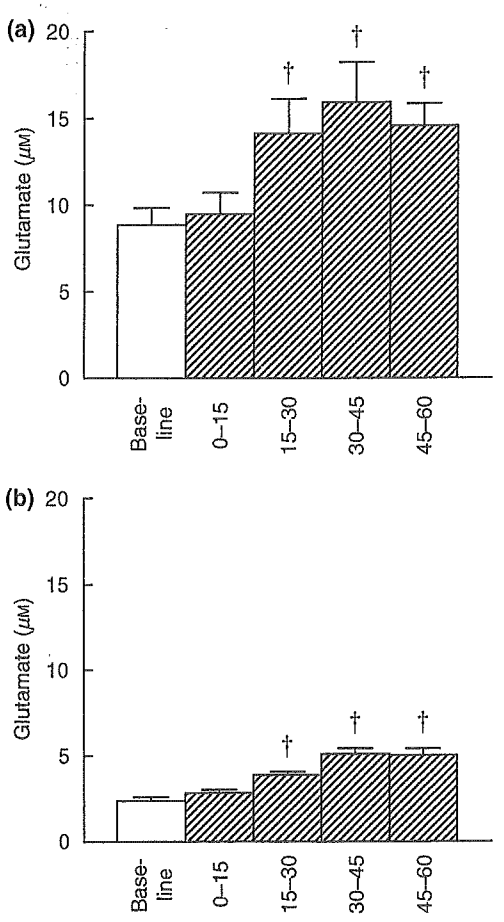

Figure 4 Changes in myocardial interstitial glutamate level in response to the local administration of ouabain without (a) and with (b) the inhibition of glutamate transporter. The glutamate level was significantly increased by ouabain administration. The ouabain-induced glutamate release was suppressed by the inhibition of glutamate transporter. Data are mean ± SE. †$P < 0.01$ from baseline.

Possible explanations for the absence of ischaemia- or ouabain-induced choline release are as follows. First, choline uptake is the rate-limiting step for ACh synthesis (Lockman & Allen 2002). Because choline in the intracellular space is rapidly consumed for ACh synthesis, the axoplasmic choline concentration might have been too low to evoke reverse transport by the choline transporter. Second, plasma choline concentration is stabilized by *de novo* choline synthesis from the catabolism of phosphatidylcholine found in cell membranes (Lockman & Allen 2002). Potential choline release may have been counterbalanced by the local stabilization mechanisms. Taking into account the recovery rate of the dialysis probe (approximately 30%), the myocardial interstitial choline concentration was 3–5 μM. Although the estimated concentration was lower than the highly regulated plasma choline concentration of approximately 10 μM, it was much higher than the ischaemia-induced maximum choline release (approximately 0.6 μM) in isolated rat hearts reported by Brühl *et al.* (2004). The present results suggest that myocardial interstitial choline level may not serve as an indicator of myocardial ischaemia in blood-perfused *in vivo* feline hearts.

By contrast with myocardial interstitial choline level, myocardial interstitial ACh level was increased both by acute myocardial ischaemia and by local administration of ouabain. Because ischaemia-induced ACh release was observed after vagal nerve transection in a previous study (Kawada *et al.* 2000), a Ca^{2+} channel-independent, regional release mechanism appears to be involved. Several reports have suggested that ouabain or ischaemia-induced intracellular Na^+ accumulation could elevate intracellular Ca^{2+} level via Na^+/Ca^{2+} exchange (Mochizuki & Jiang 1998, Li *et al.* 2000). The elevation of intracellular Ca^{2+} level may be associated with ACh release. Our previous study indicated that intracellular Ca^{2+} overload due to Ca^{2+} mobilization is responsible for the ACh release evoked by ischaemia (Kawada *et al.* 2000).

Changes in myocardial interstitial glutamate levels

Although the glutamate transporter family differs from the NA transporter family in that it requires counter-transport of K^+ instead of cotransport of Cl^-, its primary driving force is the Na^+ gradient across the plasma membrane (Schwartz 2000). Therefore, interventions that reduce the Na^+ gradient are likely to cause reverse transport of glutamate, in a similar manner to the reverse transport of NA. Acute myocardial ischaemia increased the myocardial interstitial glutamate level (Fig. 3a) as consistent with previous reports (Kennergren *et al.* 1997, 1999, Bäckström *et al.* 2003, Song *et al.* 1996). Inhibition of Na^+,K^+-ATPase also induced myocardial interstitial glutamate release (Fig. 4a). Glutamate release during acute myocardial ischaemia and local ouabain administration was significantly attenuated by the inhibition of glutamate transport (Figs 3b and 4b), suggesting the involvement of reverse transport by the glutamate transporter. Glutamate plays a vital role in keeping nitrogen balance in cells as a common amino acid in transamination reactions. The high intra-to-extracellular concentration ratio of glutamate would contribute to the retrograde transport by the glutamate transporter during the loss of normal Na^+ gradient.

In the case of myocardial interstitial NA levels, local blockade of NA uptake increased baseline NA levels, suggesting the accumulation of NA spontaneously released into the synaptic cleft (Akiyama & Yamazaki 1999). We therefore predicted that the inhibition of glutamate transport would increase the baseline gluta-

mate level. However, the inhibition of glutamate transport actually decreased the baseline glutamate level (Figs 3 and 4), suggesting that spontaneous glutamate release rather than glutamate uptake had occurred under baseline conditions. The insertion of a dialysis probe inevitably damages the myocardium. Although we waited for 2 h after implantation of the dialysis probe and the glutamate level declined with time, glutamate release from damaged myocardium may have continued. Notwithstanding this limitation, we were able to detect glutamate release in response to acute myocardial ischaemia and inhibition of Na^+,K^+-ATPase. Therefore, our interpretation that glutamate release was dependent on the reverse transport of glutamate transporter may be reasonable.

Supplementing the heart with glutamate has been shown to have beneficial effect on the recovery of contractile function in post-surgical patients (Arsenian 1998). The myocardial interstitial glutamate level remained increased during 15-min reperfusion whereas the myocardial interstitial ACh level returned towards the baseline level. Although the reason for different responses upon reperfusion was unanswered in the present study, the sustained increase in the glutamate level may have therapeutic effect on its own.

In conclusion, acute myocardial ischaemia and inhibition of Na^+,K^+-ATPase did not increase myocardial interstitial choline level despite a significant increase in myocardial interstitial ACh level. By contrast, both interventions significantly increased the myocardial interstitial glutamate level. The glutamate transporter contributed to myocardial interstitial glutamate release via retrograde transport.

This study was supported by Health and Labour Sciences Research Grant for Research on Advanced Medical Technology (H14-Nano-002) from the Ministry of Health Labour and Welfare of Japan, by Grant-in-Aid for Scientific Research (C-15590786) from the Ministry of Education, Science, Sports and Culture of Japan, and by the Program for Promotion of Fundamental Studies in Health Science of the Organization for Pharmaceutical Safety and Research from Pharmaceuticals and Medical Devices Agency (PMDA).

References

Akiyama, T. & Yamazaki, T. 1999. Norepinephrine release from cardiac sympathetic nerve endings in the in vivo ischemic region. *J Cardiovasc Pharmacol* 34(Suppl. 4), S11–S14.

Akiyama, T., Yamazaki, T. & Ninomiya, I. 1991. In vivo monitoring of myocardial interstitial norepinephrine by dialysis technique. *Am J Physiol Heart Circ Physiol* 261, H1643–H1647.

Akiyama, T., Yamazaki, T. & Ninomiya, I. 1994. In vivo detection of endogenous acetylcholine release in cat ventricles. *Am J Physiol Heart Circ Physiol* 266, H854–H860.

Arsenian, M. 1998. Potential cardiovascular applications of glutamate, aspartate, and other amino acids. *Clin Cardiol* 21, 620–624.

Bäckström, T., Goiny, M., Lockowandt, U., Liska, J. & Franco-Cereceda, A. 2003. Cardiac outflow of amino acids and purines during myocardial ischemia and reperfusion. *J Appl Physiol* 94, 1122–1128.

Brühl, A., Hafner, G. & Löffelholz, K. 2004. Release of choline in the isolated heart, an indicator of ischemic phospholipid degradation and its protection by ischemic preconditioning: no evidence for a role of phospholipase D. *Life Sci* 75, 1609–1620.

Glantz, S.A. 2002. *Primer of Biostatistics*, 5th edn. McGraw-Hill, New York.

Hearse, D.J. 1979. Oxygen deprivation and early myocardial contractile failure: a reassessment of the possible role of adenosine triphosphate. *Am J Cardiol* 44, 1115–1121.

Kawada, T., Yamazaki, T., Akiyama, T. *et al.* 2000. Differential acetylcholine release mechanisms in the ischemic and non-ischemic myocardium. *J Mol Cell Cardiol* 32, 405–414.

Kawada, T., Yamazaki, T., Akiyama, T. *et al.* 2001a. Vagosympathetic interactions in ischemia-induced myocardial norepinephrine and acetylcholine release. *Am J Physiol Heart Circ Physiol* 280, H216–H221.

Kawada, T., Yamazaki, T., Akiyama, T. *et al.* 2001b. In vivo assessment of acetylcholine-releasing function at cardiac vagal nerve terminals. *Am J Physiol Heart Circ Physiol* 281, H139–H145.

Kawada, T., Yamazaki, T., Akiyama, T. *et al.* 2002. Disruption of vagal efferent axon and nerve terminal function in the postischemic myocardium. *Am J Physiol Heart Circ Physiol* 283, H2687–H2691.

Kennergren, C., Nyström, B., Nyström, U. *et al.* 1997. In situ detection of myocardial infarction in pig by measurements of aspartate aminotransferase (ASAT) activity in the interstitial fluid. *Scand Cardiovasc J* 31, 343–349.

Kennergren, C., Mantovani, V., Lönnroth, P., Nyström, B., Berglin, E. & Hamberger, A. 1999. Extracellular amino acids as markers of myocardial ischemia during cardioplegic heart arrest. *Cardiology* 91, 31–40.

Li, S., Jiang, Q., Stys, P.K. 2000. Important role of reverse Na^+-Ca^{2+} exchange in spinal cord white matter injury at physiological temperature. *J Neurophysiol* 84, 1116–1119.

Lockman, P.R. & Allen, D.D. 2002. The transport of choline. *Drug Dev Ind Pharm* 28, 749–771.

Mochizuki, S. & Jiang, C. 1998. Na^+/Ca^{++} exchanger and myocardial ischemia/reperfusion. *Jpn Heart J* 39, 707–714.

Nicholls, D.G. 1994. *Proteins, Transmitters and Synapses*, pp. 186–199. Blackwell Science, London.

Schömig, A., Dart, A.M., Dietz, R., Mayer, E. & Kübler, W. 1984. Release of endogenous catecholamines in the ischemic myocardium of the rat. Part A: Locally mediated release. *Circ Res* 55, 689–701.

Schömig, A., Kurz, T., Richardt, G. & Schömig, E. 1988. Neuronal sodium homeostasis and axoplasmic amine concentration determine calcium-independent noradrenaline release in normoxic and ischemic rat heart. *Circ Res* 63, 214–226.

Schwartz, J.H. 2000. Neurotransmitters. In: E.R. Kandel, J.H. Schwartz & T.M. Jessell (eds) *Principles of Neural Science*, 4th edn, pp. 280–297. McGraw-Hill, New York.

Song, D., O'Regan, M.H. & Phillis, J.W. 1996. Release of the excitotoxic amino acids, glutamate and aspartate, from the isolated ischemic/anoxic rat heart. *Neurosci Lett* 220, 1–4.

Yamazaki, T., Akiyama, T., Kitagawa, H., Takauchi, Y. & Kawada, T. 1996. Elevation of either axoplasmic norepinephrine or sodium level induced release of norepinephrine from cardiac sympathetic nerve terminals. *Brain Res* 737, 343–346.

Yamazaki, T., Akiyama, T., Kitagawa, H., Takauchi, Y., Kawada, T. & Sunagawa, K. 1997. A new, concise dialysis approach to assessment of cardiac sympathetic nerve terminal abnormalities. *Am J Physiol Heart Circ Physiol* 272, H1182–H1187.

Yamazaki, T., Akiyama, T. & Kawada, T. 1999. Effects of ouabain on in situ cardiac sympathetic nerve endings. *Neurochem Int* 35, 439–445.

Cardiovascular Drugs and Therapy 19 33–40 2005

BASIC PHARMACOLOGY

Erythropoietin Just Before Reperfusion Reduces Both Lethal Arrhythmias and Infarct Size via the Phosphatidylinositol-3 Kinase-Dependent Pathway in Canine Hearts

Akio Hirata[1], Tetsuo Minamino[1], Hiroshi Asanuma[1], Shoji Sanada[1], Masashi Fujita[1], Osamu Tsukamoto[1], Masakatsu Wakeno[2], Masafumi Myoishi[2], Ken-ichiro Okada[1], Hidekazu Koyama[1], Kazuo Komamura[3], Seiji Takashima[1], Yoshiro Shinozaki[4], Hidezo Mori[3], Hitonobu Tomoike[3], Masatsugu Hori[1], and Masafumi Kitakaze[3]

[1]*Department of Internal Medicine and Therapeutics, Osaka University Graduate School of Medicine, Suita, Osaka, Japan;* [2]*Department of Bioregulatory Medicine, Osaka University Graduate School of Medicine, Suita, Osaka, Japan;* [3]*Cardiovascular Division of Internal Medicine, National Cardiovascular Center, Suita, Osaka, Japan;* [4]*Department of Physiological Science, Tokai University School of Medicine, Isehara, Kanagawa, Japan*

Summary. **Although recent studies suggest that erythropoietin (EPO) may reduce multiple features of the myocardial ischemia/reperfusion injury, the cellular mechanisms and the clinical implications of EPO-induced cardioprotection are still unclear. Thus, in this study, we clarified dose-dependent effects of EPO administered just before reperfusion on infarct size and the incidence of ventricular fibrillation and evaluated the involvement of the phosphatidylinositol-3 (PI3) kinase in the *in vivo* canine model. The canine left anterior descending coronary artery was occluded for 90 min followed by 6 h of reperfusion. A single intravenous administration of EPO just before reperfusion significantly reduced infarct size (high dose (1,000 IU/kg): 7.7 ± 1.6%, low dose (100 IU/kg): 22.1 ± 2.4%, control: 40.0 ± 3.6%) in a dose-dependent manner. Furthermore, the high, but not low, dose of EPO administered as a single injection significantly reduced the incidence of ventricular fibrillation during reperfusion (high dose: 0%, low dose: 40.0%, control: 50.0%). An intracoronary administration of a PI3 kinase inhibitor, wortmannin, blunted the infarct size-limiting and anti-arrhythmic effects of EPO. Low and high doses of EPO equally induced Akt phosphorylation and decreased the equivalent number of TUNEL-positive cells in the ischemic myocardium of dogs. These effects of EPO were abolished by the treatment with wortmannin. In conclusion, EPO administered just before reperfusion reduced infarct size and the incidence of ventricular fibrillation via the PI3 kinase-dependent pathway in canine hearts. EPO administration can be a realistic strategy for the treatment of acute myocardial infarction.**

Key Words. **erythropoietin, myocardial infarction, ventricular arrhythmia, phosphatidylinositol-3 kinase, ischemia-reperfusion injury, apoptosis**

Introduction

Recent studies have extended the traditional role of erythropoietin (EPO) from a mediator of erythroid maturation to one that provides protection against apoptotic cell death [1,2]. Recombinant human EPO (rhEPO) has been shown to exert marked protective effects against ischemia/reperfusion injury in rats and rabbits when rhEPO is administered at different time points [3–8]. Indeed, rhEPO reduced myocardial infarct size, enhanced recovery of left ventricular developed pressure, reduced the number of apoptotic cells, and induced the phosphorylation of Akt [3–8]. In these studies, high (1,000–5,000 IU/kg) doses of rhEPO, nearly 10 times higher than that used in anemic patients with chronic renal failure [9], have been applied. Recently, it was reported that phosphatidylinositol-3 (PI3) kinase

Address for correspondence: Tetsuo Minamino, MD, PhD, Department of Internal Medicine and Therapeutics, Osaka University Graduate School of Medicine, 2-2 Yamadaoka, Suita, Osaka 565-0871, Japan, Tel.: 81-6-6879-3635; Fax: 81-6-6879-3473; E-mail: minamino@medone.med.osaka-u.ac.jp

activity is required for rhEPO to recover contractile dysfunction and to block apoptosis induced by myocardial ischemia-reperfusion in isolated hearts (*ex vivo*) [10]. However, it is not determined whether rhEPO just before reperfusion reduces infarct size via PI3 kinase-dependent pathway in the *in vivo* model.

In addition to myocardial cell death, myocardial ischemia-reperfusion triggers lethal arrhythmias [11]. It is believed that at least half of the deaths due to coronary artery disease are caused by a lethal arrhythmia [12]. Although high doses of rhEPO exert cardioprotective effects against ischemia/reperfusion injury in small animals [3–8], its effects on lethal arrhythmias remain unknown. If rhEPO reduces the incidence of ventricular fibrillation (VF) in the clinical setting, there would be additional advantage to use this drug in the realistic situation of acute myocardial infarction. Thus, in the present study, we examined dose-dependent effects of rhEPO administered just before reperfusion on myocardial infarct size and the incidence of VF in the *in vivo* canine model. We also evaluated whether any such effects were mediated via the PI3 kinase pathway.

Materials and Methods

Materials

Wortmannin was obtained from Sigma (St. Louis, MO) and Phospho-Akt and Akt antibodies were obtained from Cell Signaling Technologies (Beverly, MA). RhEPO was provided by Chugai Pharmaceutical Co., Ltd (Tokyo, Japan).

Instrumentation

Forty-eight beagle dogs (Kitayama Labes, Yoshiki Farm, Gifu, Japan) weighing 8 to 12 kg were anesthetized by an intravenous injection of sodium pentobarbital (30 mg/kg), intubated, and ventilated with room air mixed with oxygen (100% O_2 at flow rate of 1.0 to 1.5 L/min). Thoracotomy was done at the left fifth intercostal space, and the heart was suspended by a pericardial cradle. After intravenous administration of heparin (500 U/kg), the left anterior descending coronary artery (LAD) was cannulated for perfusion with blood from the left carotid artery through an extracorporeal bypass tube. Coronary blood flow was measured with an electromagnetic flow probe attached to the bypass tube. We can selectively infuse drugs into LAD-perfused areas through this bypass tube. The left atrium was catheterized for microsphere injection to measure myocardial collateral blood flow during ischemia. Hydration was maintained by a slow normal saline infusion. The femoral artery was also cannulated to measure the mean systemic blood pressure (SBP). Both SBP and heart rate (HR) were monitored continuously during the study. All procedures were performed in conformity with the *Guide for the Care and Use of Laboratory Animals* (NIH Publication No. 85-23, 1996 revision), and were approved by the Osaka University Committee for Laboratory Animal Use.

Experimental protocols

Protocol 1. Long-term effects of rhEPO on hematometric parameters in dogs. To test the long-term effects of rhEPO on hematometric parameters, 100 IU/kg ($n = 5$) or 1,000 IU/kg ($n = 5$) of rhEPO was intravenously administered as a single injection. Blood was collected under pentobarbital (15 mg/kg) anesthesia before and 7, 14 days after rhEPO treatment. Hematometric parameters including hematocrit, white blood cell, and platelet counts were measured.

Protocol 2; Measurement of infarct size, coronary blood flow and myocardial collateral blood flow. After hemodynamic stabilization, we administered a low (100 IU/kg), or high (1,000 IU/kg) dose of rhEPO, or saline 10 min prior to reperfusion (n = 8–12 each) as a single intravenous injection (Fig. 1). To clarify whether rhEPO reduces myocardial infarct size through a PI3 kinase-dependent pathway, a PI3 kinase inhibitor, wortmannin, was selectively administered into the LAD (1.5 μg/kg/min) for 60 min after the onset of reperfusion. We have previously confirmed that the dose of wortmannin employed in this study is appropriate for blocking the phosphorylation of Akt in myocardium [13]. We measured infarct size and regional myocardial collateral blood flow during 90 min of ischemia as described previously [14]. In brief, infarct size was evaluated at the end of the protocol by Evans blue/TTC staining, while collateral blood flow was assessed by the non-radioactive microsphere method [14]. Coronary blood flow was monitored continuously during the study. To ensure that all of the animals included in the data analysis were healthy and were exposed to a similar extent of ischemia, the exclusion criteria reported previously for excessive myocardial collateral blood flow (>15 mL/100 g/min) and lethal arrhythmia (more than two consecutive attempts required to convert VF with low-energy DC pulses applied directly to the heart) were adopted [14].

Effects of rhEPO on VF during reperfusion period

In Protocol 2, we also evaluated the incidence of VF during the 6 h reperfusion period (Fig. 1). Since myocardial collateral blood flow during ischemia exhibited a negative correlation with the incidence of VF [15,16], the dogs with excessive collateral blood flow (>15 mL/100 g/min) were excluded from VF analysis.

Phosphorylation of Akt

We used 12 dogs for western blot in the control, low EPO, high EPO, and high EPO + WTMN groups ($n = 3$ each) in Protocol 2 (Fig. 1). After 90 min of ischemia followed by 6 h of reperfusion, hearts were excised and

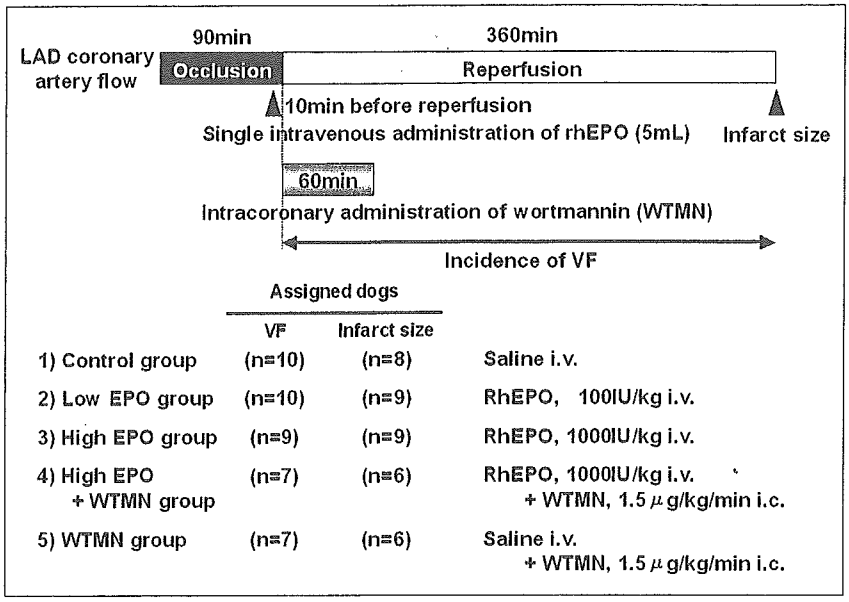

Fig. 1. *Experimental protocol for infarct size and VF.*

the myocardial tissue in the ischemic zone was quickly placed into liquid nitrogen and stored at −80°C. Phosphorylation of Akt and total content of Akt were evaluated as reported previously [13]. The immunoreactive bands were quantified by densitometry (Molecular Dynamics).

Terminal deoxynucleotidyl transferase-mediated dUTP nick-end labeling (TUNEL)

In Protocol 2, the myocardial tissue samples were taken from the ischemic zone of dogs in the control, low EPO, high EPO, and high EPO + WTMN groups ($n = 3$ each). These were fixed in 10% buffered formalin, embedded in paraffin, and serially sectioned in the frontal plane at 5-μm thickness. Analysis by TUNEL method was performed according to the protocol supplied with the in situ apoptosis detection kit, the Apop Tag Peroxidase *In Situ* Apoptosis Detection Kit (CHEMICON International, USA). TUNEL-positive cell nuclei and total cell nuclei stained metylgreen were counted in 10–15 random high-power fields (×400), and the percentage of TUNEL-positive cell nuclei to total cell nuclei ($n =$ 1,000) were then calculated.

Statistical analysis

Statistical analysis was performed by one-way factional analysis of variance (ANOVA) with modified Bonferroni's post hoc test when the data were compared among groups. Time courses of the changes were compared by repeated measures ANOVA. The incidence of VF was compared using the χ^2-test and Fisher's exact probability test. Results were expressed as the mean ± SEM, with $p < 0.05$ considered significant.

Results

The long-term effects of rhEPO on hematometric parameters

The single administration of either 100 IU/kg or 1,000 IU/kg of rhEPO did not change any hematometric parameters including hematocrit, white blood cells, and platelet counts 7 or 14 days after rhEPO treatment (Table 1).

Table 1. *Long-term effects of rhEPO on hematometric parameters in dogs*

	EPO 100 IU/kg			EPO 1000 IU/kg		
Parameters	Day 0	Day 7	Day 14	Day 0	Day 7	Day 14
Ht (%)	50.1 ± 0.8	51.1 ± 0.9	51.3 ± 1.0	51.5 ± 1.3	52.0 ± 1.0	53.1 ± 0.7
WBC ($10^3/\mu$L)	11.7 ± 1.3	12.1 ± 0.7	11.4 ± 0.6	11.5 ± 1.3	11.7 ± 0.7	12.0 ± 1.0
Platelet (10^4/mm^3)	33.7 ± 2.0	33.7 ± 1.8	33.3 ± 1.7	33.2 ± 1.9	34.0 ± 2.4	36.4 ± 3.4

Data are presented as Mean ± SEM. $n = 5$.

Abbreviations: rhEPO = recombinant human erythropoietin, Ht = hematocrit, WBC = white blood cell.

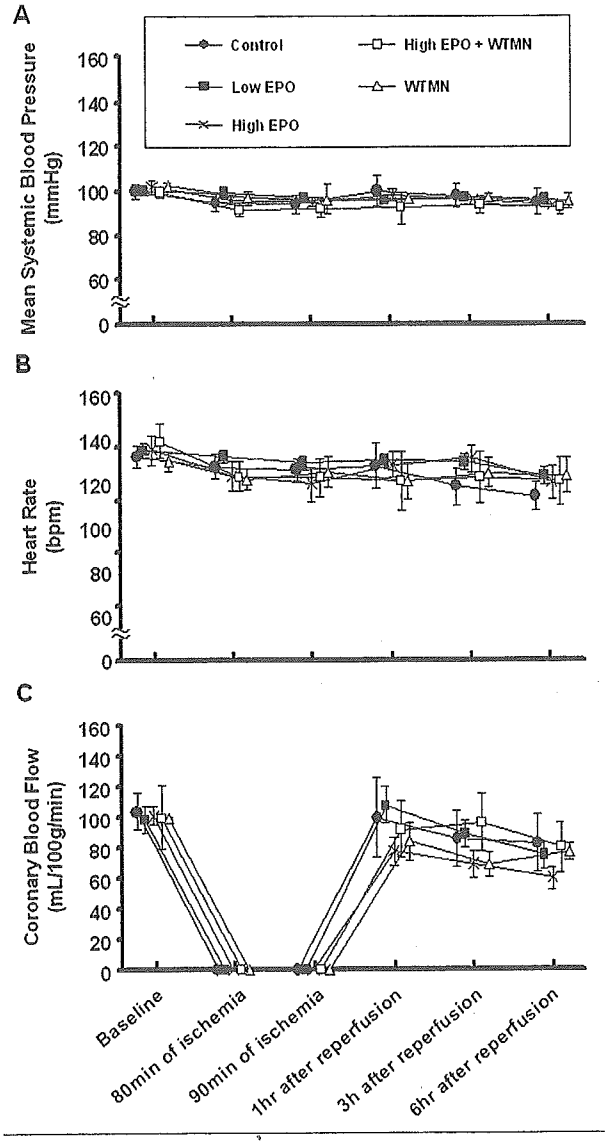

Fig. 2. The changes in mean systemic blood pressure, heart rate and coronary blood flow during the experiment in groups tested.

Effects of rhEPO on infarct size and VF during the reperfusion period

Since 5 of 48 dogs were excluded from analysis because of excessive collateral blood flow (>15 mL/100 g/min) (control: 1, low EPO: 2, high EPO: 1, high EPO + WTMN: 0, WTMN: 1), 43 dogs were evaluated for VF analysis. Among these 43 dogs, we excluded 5 dogs (control: 2, low EPO: 1, high EPO: 0, high EPO + WTMN: 1, WTMN: 1) that matched the exclusion criteria of lethal arrhythmia from infarct size analysis.

Throughout the study, neither SBP (Fig. 2A), nor HR (Fig. 2B), nor coronary blood flow (Fig. 2C) differed among the 5 groups. The area at risk (Fig. 3A) and myocardial collateral blood flow in the LAD region during myocardial ischemia (Fig. 3B) were also comparable in the groups tested.

Table 2. Effects of rhEPO on the incidence of VF during reperfusion periods

Group	Incidence of VF	
Control	50.0%	(5/10)
Low EPO	40.0%	(4/10)
High EPO	0%*	(0/9)
High EPO + WTMN	42.9%	(3/7)
WTMN	42.9%	(3/7)

*$p < 0.05$ vs. control group.
Abbreviations: VF = ventricular fibrillation, rhEPO = recombinant human erythropoietin, WTMN = wortmannin.

Figure 4 shows infarct size in the groups tested. A low or high dose of rhEPO significantly ($p < 0.05$) reduced the infarct size compared with that in the control group. Furthermore, a high dose of rhEPO reduced infarct size more than a low dose of rhEPO did. The intracoronary administration of wortmannin for 60 min after the onset of reperfusion abrogated the infarct-limiting effect of rhEPO, although wortmannin alone did not affect infarct size.

The high, but not low, dose of rhEPO significantly ($p < 0.05$) reduced the incidence of VF during the 6 h reperfusion period compared with the control. The antiarrhythmic effects of rhEPO were abolished by wortmannin (Table 2).

Effects of rhEPO on Akt phosphorylation

After 90 min of ischemia followed by 6 h of reperfusion, the ratio of phosphorylated Akt to total Akt in the low and high EPO groups significantly ($p < 0.05$) increased compared with that in the control group. The increase in this ratio was completely abolished by the treatment with wortmannin (Fig. 5).

Effects of rhEPO on apoptosis

The ratio of TUNEL positive cells to total cells in the low and high EPO groups decreased compared with that in the control group. The reduction of TUNEL-positive cells by rhEPO was completely abolished by the treatment with wortmannin (Fig. 6).

Discussion

In this study, we demonstrated that a single intravenous administration of rhEPO just before reperfusion limited not only infarct size but also the incidence of VF. Moreover, our data suggest that the infarct size-limiting and anti-arrhythmic effects of rhEPO were through the PI3 kinase-dependent pathways in the *in vivo* canine hearts.

Important considerations towards clinical application of rhEPO are the timing and dose of its administration. The previous studies reported that rhEPO administered at the onset of reperfusion [7,8] as well

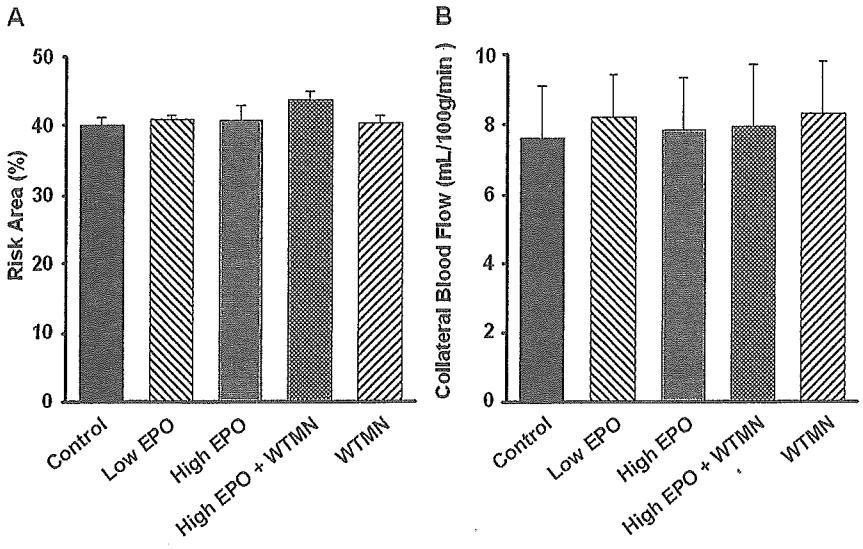

Fig. 3. Area at risk and myocardial collateral blood flow during ischemia in groups tested.

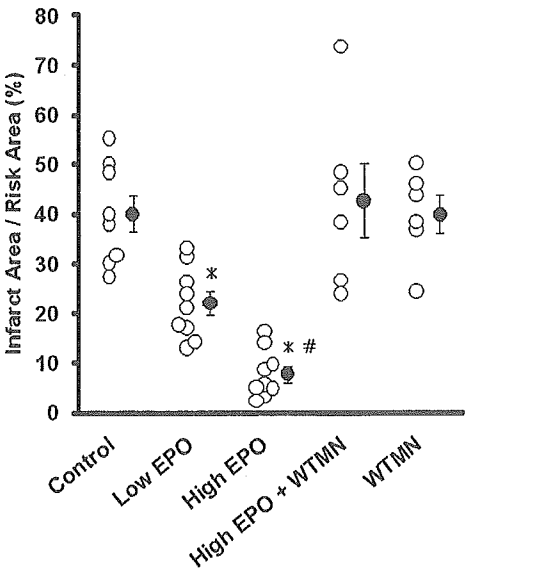

*Fig. 4. Infarct size in groups tested. *p < 0.05 vs. control group. #p < 0.05 vs. low EPO group. Open circles show the infarct size in each individual.*

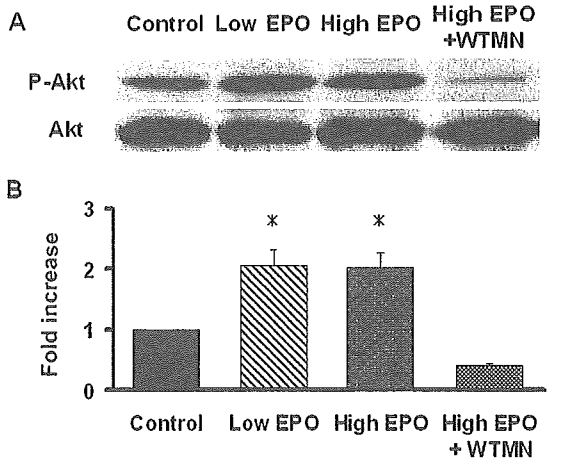

*Fig. 5. Phosphorylation of Akt in canine hearts. (A) Representative Western blot for phosphorylated and total Akt. (B) Densitometry graphs indicating fold expression over control for Akt. n = 3 each. *p < 0.05 vs. control group.*

as ischemia [7,8] reduces infarct size in rabbit and rat hearts. Consistent with these reports, we confirmed that rhEPO administered 10 min before reperfusion reduced myocardial infarct size in dogs. Our findings support the idea that in humans the adjunctive therapy with rhEPO treatment during coronary intervention would reduce myocardial infarct size.

The doses of rhEPO (1,000–5,000 IU/kg) administered in previous experimental studies [3–8] were nearly 10 times higher than those clinically used in anemic patients with chronic renal failure [9]. In the present study, we demonstrated that both 100 IU/kg and 1,000 IU/kg of rhEPO as a single administration significantly reduced myocardial infarct size, although a high dose of rhEPO significantly reduced infarct size more than a low dose of rhEPO did. This finding suggests that the clinically relevant dose of rhEPO used in patients with chronic renal failure can reduce myocardial infarct size. In the previous clinical studies, a high dose (33,000 IU once daily for the first 3 days) of intravenously administered rhEPO was well tolerated in patients with stroke and improved clinical outcome at 1 month [17]. On the other hand, a high dose (40,000–60,000 IU per week) of subcutaneously administered rhEPO, while not as a single injection,

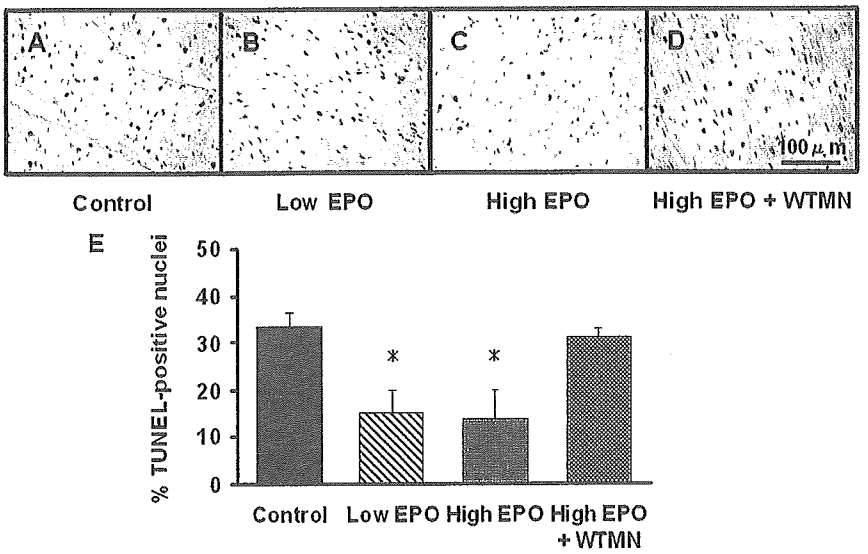

*Fig. 6. TUNEL staining in canine hearts after 90 min ischemia followed by 6 h of reperfusion. Representative examples of TUNEL-staining from canine hearts in the control (A), low EPO (B), high EPO (C), and high EPO + WTMN groups (D). (E) Quantitative data of the percentage of TUNEL-positive nuclei to total cell nuclei. *p < 0.05 vs. control group.*

increased the incidence of thrombotic events such as deep venous thrombosis or pulmonary embolisms in patients with breast cancer [18]. Furthermore, there are some reports that rhEPO increases the number of platelets in normal rats [19] and chronically hemodialyzed patients [20]. In the present study, we didn't find that either low or high dose of rhEPO, as a single injection, changed hematometric parameters. Although these findings suggest that a single administration of 1,000 IU/kg of rhEPO, that induced marked reduction of myocardial infarct size, could be used safely, we must be careful for the use of a high dose of rhEPO for the treatment of myocardial infarction.

Previous reports have shown that both phosphorylation of Akt and inhibition of apoptosis are associated with infarct size-limiting effects due to rhEPO [4,6–8]. Recently, it was reported that PI3 kinase activity is required for rhEPO to recover contractile dysfunction and to block apoptosis induced by myocardial ischemia-reperfusion in isolated hearts (*ex vivo*) [10]. Although the recovery of contractile function could be related to the reduction of infarct size, no evidence was presented that rhEPO reduced infarct size via the PI3 kinase-dependent pathway. In the present study we have demonstrated that the infarct size-limiting effect of rhEPO was blunted by the intracoronary administration of wortmannin in dogs. This is the first evidence showing that the infarct size-limiting effect of rhEPO is dependent on the PI3 kinase pathway in *in vivo* hearts.

In the present study, low and high doses of rhEPO equally increased phosphorylation of Akt and decreased equivalent number of TUNEL-positive cells in the ischemic myocardium of dogs. Either Akt phosphorylation or a decrease in the number of TUNEL-positive cells was prevented by the PI3 kinase inhibitor, wortmannin. This finding suggests that rhEPO prevents apoptotic cell death through PI3 kinase/Akt-dependent pathway in canine hearts. However, since the TUNEL method also detects single strand breaks occurring in the course of necrotic cell death [21], it is likely that rhEPO attenuates apoptotic and necrotic cell death. Indeed, if rhEPO only inhibits the apoptotic cell death, it may be difficult to explain the marked reduction of infarct size by rhEPO. Interestingly, the previous studies reported that the PI3 kinase activates not only Akt but also protein kinase C or mitogen-activated protein kinase in ischemia/reperfusion models [22–24], either of which mediates the cellular protection against necrotic process [25,26]. Furthermore, recent reports suggest that rhEPO can inhibit the release of free radicals from neutrophils [27] and act as a radical scavenger [28], both of which may reduce cardiac cell death after ischemia/reperfusion. Although further investigation will be needed, these characteristics of rhEPO may contribute to the reduction of necrotic as well as apoptotic cell death in ischemia/reperfused myocardium. In addition, since wortmannin inhibits not only PI3 kinase but also PI4 kinase and PI kinase related protein kinase, there is a limitation in using wortmannin as a specific inhibitor of PI3 kinase [29].

In clinical settings, ventricular arrhythmias are often observed in patients following reperfusion therapy and they can be life-threatening [30]. Importantly, the present study demonstrated that a high, but not a low dose of rhEPO prevented VF during reperfusion via the PI3 kinase-dependent pathway. Since low and high doses of rhEPO equally increased phosphorylation of Akt, it is unlikely that Akt is responsible for

the rhEPO-induced anti-arrhythmic effect. There are several possible mechanisms by which rhEPO exerts anti-arrhythmic effects via the PI3 kinase-dependent, but Akt-independent, pathway. First, under conditions of reperfusion, production of inositol-1,4,5-trisphospate (IP3) increases when phospholipase C (PLC) is activated through α-adrenoreceptors on the myocardial cell membrane [11]. This increase in IP3 activates IP3 receptors on the sarcoplasmic reticulum causing the release of Ca^{2+}. The increases in the intracellular Ca^{2+} levels caused by IP3 have been reported to initiate slow Ca^{2+} oscillations, which underlies the delayed afterdepolarizations that trigger many arrhythmias including VF [11,31]. PLC hydrolyzes phosphatidylinositol-4,5-bisphospate (PIP2) to produce IP3. Since PI3 kinase and PLC can act upon the common substrate, PIP2 [32], rhEPO may prevent lethal arrhythmia by activating the PI3 kinase pathway that results in the decrease in PIP2 levels, which will lead to prevent Ca^{2+} overload by IP3. Second, since oxygen-derived free radicals are involved in the generation of reperfusion arrhythmia [30,33,34], rhEPO may decrease reperfusion arrhythmia through the prevention of free radicals release from neutrophils or acting as a radical scavenger [27,28]. Finally, we need to consider that rhEPO exerts anti-arrhythmic effects by the reduction of myocardial infarct size.

In conclusion, our findings, when translated into clinical practice, may support the use of rhEPO as a cardioprotective agent in the treatment of patients with myocardial infarction.

Acknowledgments

We thank Yuko Okuda, Yoko Nagamachi, Nobuko Kawasaki and Tomi Fukushima for their technical assistance.

References

1. Siren AL, Fratelli M, Brines M, et al. Erythropoietin prevents neuronal apoptosis after cerebral ischemia and metabolic stress. *Proc Natl Acad Sci USA* 2001;98:4044–4049.
2. van der Meer P, Voors AA, Lipsic E, van Gilst WH, van Veldhuisen DJ. Erythropoietin in cardiovascular diseases. *Eur Heart J* 2004;25:285–291.
3. Calvillo L, Latini R, Kajstura J, et al. Recombinant human erythropoietin protects the myocardium from ischemia-reperfusion injury and promotes beneficial remodeling. *Proc Natl Acad Sci USA* 2003;100:4802–4806.
4. Tramontano AF, Muniyappa R, Black AD, et al. Erythropoietin protects cardiac myocytes from hypoxia-induced apoptosis through an Akt-dependent pathway. *Biochem Biophys Res Commun* 2003;308:990–994.
5. Moon C, Krawczyk M, Ahn D, et al. Erythropoietin reduces myocardial infarction and left ventricular functional decline after coronary artery ligation in rats. *Proc Natl Acad Sci USA* 2003;100:11612–11617.
6. Parsa CJ, Matsumoto A, Kim J, et al. A novel protective effect of erythropoietin in the infarcted heart. *J Clin Invest* 2003;112:999–1007.
7. Parsa CJ, Kim J, Riel RU, et al. Cardioprotective effects of erythropoietin in the reperfused ischemic heart: A potential role for cardiac fibroblasts. *J Biol Chem* 2004;279:20655–20662.
8. Lipsic E, van der Meer P, Henning RH, et al. Timing of erythropoietin treatment for cardioprotection in ischemia/reperfusion. *J Cardiovasc Pharmacol* 2004;44:473–479.
9. NKF-DOQI clinical practice guidelines for the treatment of anemia of chronic renal failure. National Kidney Foundation-Dialysis Outcomes Quality Initiative. *Am J Kidney Dis* 1997;30:S192–S240.
10. Cai Z, Semenza GL. Phosphatidylinositol-3-kinase signaling is required for erythropoietin-mediated acute protection against myocardial ischemia/reperfusion injury. *Circulation* 2004;109:2050–2053.
11. Woodcock EA, Matkovich SJ, Binah O. Ins(1,4,5)P3 and cardiac dysfunction. *Cardiovasc Res* 1998;40:251–256.
12. Billman GE, Hallaq H, Leaf A. Prevention of ischemia-induced ventricular fibrillation by omega 3 fatty acids. *Proc Natl Acad Sci USA* 1994;91:4427–4430.
13. Ogita H, Node K, Asanuma H, et al. Raloxifene improves coronary perfusion, cardiac contractility, and myocardial metabolism in the ischemic heart: Role of phosphatidylinositol 3-kinase/Akt pathway. *J Cardiovasc Pharmacol* 2004;43:821–829.
14. Ogita H, Node K, Asanuma H, et al. Amelioration of ischemia- and reperfusion-induced myocardial injury by the selective estrogen receptor modulator, raloxifene, in the canine heart. *J Am Coll Cardiol* 2002;40:998–1005.
15. Hale SL, Lange R, Alker KJ, Kloner RA. Correlates of reperfusion ventricular fibrillation in dogs. *Am J Cardiol* 1984;53:1397–1400.
16. Bolli R, Patel B. Factors that determine the occurrence of reperfusion arrhythmias. *Am Heart J* 1988;115:20–29.
17. Ehrenreich H, Hasselblatt M, Dembowski C, et al. Erythropoietin therapy for acute stroke is both safe and beneficial. *Mol Med* 2002;8:495–505.
18. Rosenzweig MQ, Bender CM, Lucke JP, Yasko JM, Brufsky AM. The decision to prematurely terminate a trial of R-HuEPO due to thrombotic events. *J Pain Symptom Manage* 2004;27:185–190.
19. Berridge MV, Fraser JK, Carter JM, Lin FK. Effects of recombinant human erythropoietin on megakaryocytes and on platelet production in the rat. *Blood* 1988;72:970–977.
20. Tang WW, Stead RA, Goodkin DA. Effects of Epoetin alfa on hemostasis in chronic renal failure. *Am J Nephrol* 1998;18:263–273.
21. Ohno M, Takemura G, Ohno A, et al. "Apoptotic" myocytes in infarct area in rabbit hearts may be oncotic myocytes with DNA fragmentation: Analysis by immunogold electron microscopy combined with In situ nick end-labeling. *Circulation* 1998;98:1422–1430.
22. Mizukami Y, Hirata T, Yoshida K. Nuclear translocation of PKC zeta during ischemia and its inhibition by wortmannin, an inhibitor of phosphatidylinositol 3-kinase. *FEBS Lett* 1997;401:247–251.
23. Mizukami Y, Kobayashi S, Uberall F, Hellbert K, Kobayashi N, Yoshida K. Nuclear mitogen-activated protein kinase activation by protein kinase czeta during reoxygenation after ischemic hypoxia. *J Biol Chem* 2000;275:19921–19927.

24. Takeda H, Matozaki T, Takada T, et al. PI 3-kinase gamma and protein kinase C-zeta mediate RAS-independent activation of MAP kinase by a Gi protein-coupled receptor. *Embo J* 1999;18:386–395.
25. Ping P, Zhang J, Zheng YT, et al. Demonstration of selective protein kinase C-dependent activation of Src and Lck tyrosine kinases during ischemic preconditioning in conscious rabbits. *Circ Res* 1999;85:542–550.
26. Sanada S, Kitakaze M, Papst PJ, et al. Role of phasic dynamism of p38 mitogen-activated protein kinase activation in ischemic preconditioning of the canine heart. *Circ Res* 2001;88:175–180.
27. Kristal B, Shurtz-Swirski R, Shasha SM, et al. Interaction between erythropoietin and peripheral polymorphonuclear leukocytes in hemodialysis patients. *Nephron* 1999;81:406–413.
28. Chattopadhyay A, Choudhury TD, Bandyopadhyay D, Datta AG. Protective effect of erythropoietin on the oxidative damage of erythrocyte membrane by hydroxyl radical. *Biochem Pharmacol* 2000;59:419–425.
29. Stein RC. Prospects for phosphoinositide 3-kinase inhibition as a cancer treatment. *Endocr Relat Cancer* 2001;8:237–248.
30. Jeroudi MO, Hartley CJ, Bolli R. Myocardial reperfusion injury: Role of oxygen radicals and potential therapy with antioxidants. *Am J Cardiol* 1994;73:2B–7B.
31. Van Wagoner DR, Bond M. Reperfusion arrhythmias: New insights into the role of the Na(+)/Ca(2+) exchanger. *J Mol Cell Cardiol* 2001;33:2071–2074.
32. Marshall AJ, Niiro H, Yun TJ, Clark EA. Regulation of B-cell activation and differentiation by the phosphatidylinositol 3-kinase and phospholipase Cgamma pathway. *Immunol Rev* 2000;176:30–46.
33. Lee YM, Hsiao G, Chen HR, Chen YC, Sheu JR, Yen MH. Magnolol reduces myocardial ischemia/reperfusion injury via neutrophil inhibition in rats. *Eur J Pharmacol* 2001;422:159–167.
34. Hansen PR. Myocardial reperfusion injury: Experimental evidence and clinical relevance. *Eur Heart J* 1995;16:734–740.

Am J Physiol Heart Circ Physiol 289: H924–H930, 2005.
First published April 15, 2005; doi:10.1152/ajpheart.01207.2004.

Microdialysis separately monitors myocardial interstitial myoglobin during ischemia and reperfusion

Hirotoshi Kitagawa,[1] Toji Yamazaki,[2] Tsuyoshi Akiyama,[2] Masaru Sugimachi,[3] Kenji Sunagawa,[4] and Hidezo Mori[2]

[1]*Department of Anesthesiology, Shiga University of Medical Science, Otsu; Departments of* [2]*Cardiac Physiology and* [3]*Cardiovascular Dynamics, National Cardiovascular Center Research Institute, Suita; and* [4]*Department of Cardiovascular Medicine, Kyushu University Graduate School of Medical Sciences, Fukuoka, Japan*

Submitted 1 December 2004; accepted in final form 6 April 2005

Kitagawa, Hirotoshi, Toji Yamazaki, Tsuyoshi Akiyama, Masaru Sugimachi, Kenji Sunagawa, and Hidezo Mori. Microdialysis separately monitors myocardial interstitial myoglobin during ischemia and reperfusion. *Am J Physiol Heart Circ Physiol* 289: H924–H930, 2005. First published April 15, 2005; doi:10.1152/ajpheart.01207.2004.—Direct monitoring of myoglobin efflux during ischemia and reperfusion has been limited because of inherent sample collection problems in the ischemic region. Recently, the cardiac dialysis technique has offered a powerful method for monitoring myocardial interstitial levels of low-molecular-weight compounds in the cardiac ischemic region. In the present study, we extended the molecular target to high-molecular-weight compounds by use of microdialysis probes with a high-molecular-mass cutoff and monitored myocardial interstitial myoglobin levels. A dialysis probe was implanted in the left ventricular free wall in anesthetized rabbits. The main coronary artery was occluded for 60 or 120 min. We examined the effects of myocardial ischemia and reperfusion on myocardial interstitial myoglobin levels. Interstitial myoglobin increased within 15 min of ischemia and continued to increase during 120 min of ischemia, whereas blood myoglobin increased at 45 min of ischemia. Lactate and myoglobin in the interstitial space increased during the same period. At 60 min of ischemia, reperfusion markedly accelerated interstitial myoglobin release. The interstitial myoglobin level was fivefold higher at 0–15 min of reperfusion than at 60–75 min of coronary occlusion. The dialysis technique permits earlier detection of myoglobin release and separately monitors myoglobin release during ischemia and reperfusion. Myocardial interstitial myoglobin levels can serve as an index of myocardial injury evoked by ischemia or reperfusion.

infarction; interstitial space; membrane permeability

IT IS WELL KNOWN that certain proteins, including myoglobin, called serum cardiac markers, are released into the bloodstream in large quantities from necrotic cardiac muscle cells after myocardial infarction (20, 26, 43). However, because direct samples from the ischemic region are not readily obtainable, in situ studies on efflux of these proteins in the cardiac ischemic region have been limited (22). This problem of sample collection from the ischemic region remains unresolved. First, it is uncertain exactly when cardiac markers appear from injured myocardium. The appearance of cardiac markers indicates the turning point from reversible injury to irreversible damage (43). However, the first appearance of cardiac markers in the bloodstream is influenced by the slow transport of cardiac markers from the interstitial space into the bloodstream (20). Thus the detection of this appearance is of great value in understanding the pathophysiological events induced by myocardial ischemia. Second, recent experimental and clinical findings suggest that reperfusion itself seems to accelerate the release of cardiac markers (18, 37, 38). However, the extent to which reperfusion contributes to relative changes in their release is unclear. To determine myocardial injury evoked by reperfusion, more information is needed about the extent to which ischemia and reperfusion affect changes in the release of cardiac markers. Third, present methods used to measure infarct size require tissue analysis several hours after the ischemic event (8). Furthermore, histochemical analysis depends on the times of ischemia and reperfusion (23, 33). Concise, dissociated assessments of ischemia and reperfusion injury have been a frequent object of research.

In general, mobilization of cardiac markers from ischemic myocardium to the bloodstream has been divided into two different sequences: release from the myocardial cell to the interstitial space and transport from the interstitial space into the bloodstream (20). Therefore, if we examine the first process in in situ myocardium, we can discuss the pathophysiological changes during development of ischemic myocardial necrosis. However, little information is available on interstitial protein kinetics in the ischemic region (15). Examination of protein kinetics in the ischemic region has been limited to assessment of protein kinetics in the isolated Langendorff-perfused heart (28, 39). Recently, a cardiac dialysis technique has provided a powerful method for monitoring myocardial interstitial levels of low-molecular-weight compounds in the cardiac ischemic region (2, 6, 14, 31). Furthermore, this method is suitable for distinguishing between ischemia and reperfusion responses (32). By improving the microdialysis probes with a high-molecular-mass cutoff membrane, we have extended the molecular target to high-molecular-weight peptides and proteins and monitored myocardial interstitial protein levels.

In the present study, we chose myoglobin as one of the earliest biochemical markers in myocardial injury (4, 34). We applied the dialysis technique to the heart of anesthetized rabbits and investigated myocardial interstitial myoglobin levels during coronary occlusion and reperfusion. To address the above-mentioned issues, we compared the first appearance of myocardial interstitial myoglobin levels with that of low-molecular-weight metabolites (lactate and glycerol). Further-

Address for reprint requests and other correspondence: T. Yamazaki, Dept. of Cardiac Physiology, National Cardiovascular Center Research Institute, 5-7-1 Fujishirodai, Suita, Osaka 565-8565, Japan (E-mail: yamazaki@ri.ncvc.go.jp).

The costs of publication of this article were defrayed in part by the payment of page charges. The article must therefore be hereby marked "*advertisement*" in accordance with 18 U.S.C. Section 1734 solely to indicate this fact.